



**HAL**  
open science

## Effect of thermomechanical couplings on viscoelastic behaviour of polystyrene

Pankaj Yadav, Andre Chrysochoos, Olivier Arnould, Sandrine Bardet

► **To cite this version:**

Pankaj Yadav, Andre Chrysochoos, Olivier Arnould, Sandrine Bardet. Effect of thermomechanical couplings on viscoelastic behaviour of polystyrene. SEM 2019 - Annual Conference and Exposition on Experimental and Applied Mechanics, Jun 2019, Reno, United States. hal-02088717

**HAL Id: hal-02088717**

**<https://hal.science/hal-02088717>**

Submitted on 3 Apr 2019

**HAL** is a multi-disciplinary open access archive for the deposit and dissemination of scientific research documents, whether they are published or not. The documents may come from teaching and research institutions in France or abroad, or from public or private research centers.

L'archive ouverte pluridisciplinaire **HAL**, est destinée au dépôt et à la diffusion de documents scientifiques de niveau recherche, publiés ou non, émanant des établissements d'enseignement et de recherche français ou étrangers, des laboratoires publics ou privés.

# Effect of thermomechanical couplings on viscoelastic behaviour of polystyrene

Pankaj Yadav, Graduate Student  
André Chrysochoos, Professor  
Olivier Arnould, Asst. Professor  
Sandrine Bardet, Asst. Professor  
Laboratory of Mechanics and Civil Engineering  
Montpellier University, CNRS Montpellier  
34090, France

## ABSTRACT

Analysis of the thermo-mechanical behaviour of the polymers has been and still is the subject of many rheological studies both experimentally and theoretically. For small deformations, the modelling framework retained by rheologists is often of linear viscoelasticity which led us to the definition of complex moduli and to the rules of the renowned time-temperature superposition principle (TTSP). In this context, the effect of time (i.e., rate dependence) is almost unanimously associated with viscous effects. It has however been observed that the dissipative effects associated with viscous effects may be superimposed with thermo-elastic coupling effects, indicating a high sensitivity of polymeric materials to temperature variations (thermodilatibility). Indeed, because of heat diffusion, it was also noticed that these strong thermo-mechanical couplings may induce a time dependence of the material behaviour. Using traditional experimental methods of visco-analysis i.e., dynamic mechanical thermal analysis (DMTA) and via an experimental energy analysis of the behaviour using quantitative infrared techniques, the relative importance of thermoelastic heat sources compared to viscous dissipation was analysed with the increasing frequency of monochromatic cyclic tensile tests made at different ambient temperatures.

## Keywords

Time-temperature superposition (TTSP), viscoelasticity, dissipation, thermo-mechanical coupling, DMTA.

## Introduction

Polymeric materials are widely known for their high viscoelasticity, which signifies wide dependence of their mechanical responses on the applied strain rate which is very important in duration for numerous engineering applications. This is one of the reasons why a protocol capable of predicting the viscoelastic behaviour of polymeric materials over time scales and temperatures of use has been developed. This protocol gave rise to DMTA techniques which allow to gather viscoelastic behaviour characteristics at easily adaptable frequencies and temperature of use in laboratories and extrapolate them to very large ranges of strain rate and temperatures. During the DMTA tests, a monochromatic sinusoidal signal is applied on the specimen to observe the stress-strain response and derive the so called dynamic moduli i.e.,  $E'$  and  $E''$  respectively named as storage and loss moduli. In general, the storage modulus is associated with the stored elastic energy which is recoverable during unloading while the loss modulus is supposed to be associated with the viscous dissipated energy. The viscous part of the behaviour is equivalently characterised by the loss tangent defined by  $\tan \delta = E''/E'$  [1]. The DMTA constitutive equations can then be summarized as follows:

$$\begin{cases} \varepsilon = \varepsilon_0 \sin \omega t \\ \sigma = \sigma_0 \sin(\omega t + \delta) = E' \sin \omega t + E'' \cos \omega t \\ E' = \sigma_0 / \varepsilon_0 \cos \delta \\ E'' = \sigma_0 / \varepsilon_0 \sin \delta \end{cases} \quad (1)$$

where  $\varepsilon_0$  is the loading amplitude,  $\sigma_0$  the stress amplitude and  $\omega=2\pi f$ , the pulsation and  $f$  being the loading frequency.

Mechanical tests, performed at constant ambient temperature and carried at several frequencies (also known as frequency sweep), permit the investigation of viscoelastic characteristics on a small time scale equivalent to few decades. According to the literature, the assessments, extracted from tests carried out at different frequencies and constant ambient temperature, show the same evolutions of  $E'$  and  $E''$  as one of the isochronal tests conducted at different ambient temperatures [2]. This similar behaviour is in accordance with the fact that the relaxation times of the molecular processes will be short, hence more relaxation can take place over the time-scale associated with the strain controlled loading. On the other side, the same observation would be made at low frequencies, where the time-scale associated with the strain controlled loading is long and similarly, more stress relaxation can take place. This implies that the variation of temperature corresponds to a shift in time scale and this relation between time (or loading frequency) and temperature is termed as time-temperature superposition principle [3] and is known to be valid only for “thermorheologically simple” materials. These are the materials which shows that the variation of temperature corresponds to a shift in time scale [4]. For example, considering a given relaxation time  $\tau$ , its changes with the temperature then introduce a shift factor  $a_T$  such that:

$$\tau(T) = \frac{\tau(T_0)}{a_T(T)} \quad (2)$$

According to equation 1, the linear viscoelastic behaviour of materials lead us to show stabilized hysteretic responses (stress-strain loops) whose area corresponds to the mechanical energy lost in form of the dissipated mechanical energy over a cycle, often leading to a self-heating of the specimen. The intensity of the self-heating naturally depends on the material characteristics, on the loading frequency and on the thermal boundary conditions. However, Zener [5] observed that the stress-strain loop may not only be induced by the dissipation mechanisms but also by thermoelastic effects. For all purposes, a theoretical thermodynamic description of these “thermoelastic damping” can be found in [6].

This present work analysed the experimental results obtained from DMTA device equipped with an Infrared camera. The Infrared data were used to estimate the temperature variations of the specimen during the cyclic loading in order to detect the possible thermo-mechanical coupling and/or dissipative effects. The outputs of the different tests are discussed in terms of energy balance. This paper also presents an analytical way to derive the concept of thermorheologically simple materials used in the DMTA protocol within a thermomechanical viscoelastic framework where the status of the temperature is the one of a controlled parameter but not (yet) those of a thermodynamic variable.

## Experimental Methods

Firstly, the standard DMTA setup used for polystyrene samples was shown followed by the experimental home-made arrangement developed to allow us to perform a thermographic analysis during the DMTA tests.

### (a) Standard DMTA

The polystyrene (PS) had a molecular weight ( $M_n$ ) of 36,276 and a polydispersity of 3.072, was used to carry out the DMTA tests. The samples of dimension 85x13x4 mm were made from the sheets (300 x 300mm) of PS from Goodfellow to characterize the viscoelastic behaviour using the DMTA technique. The tests were made on a classical DMTA (BOSE ELF 3230) equipped with strain control module (Figure 1). The samples were tested in the temperature range from 40°C to 90°C and for 3 decades of frequency from 0.01 Hz to 10 Hz i.e., frequency sweep was made with 5 points per decade in the tension

mode with a strain ratio of  $R = -1$ . A virgin sample was utilized for each new loading parameter to avoid possible damage or ageing [7]

The glass transition temperature of PS samples, measured using the Dynamic Scanning Calorimetry (DSC) was  $108^{\circ}\text{C}$ . This glass transition temperature value was not the exact value of glass transition but was an adequate value for us to stay below the glass transition region.

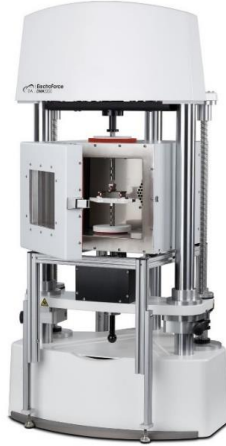


Fig.1 BOSE Electroforce 3230 DMTA equipped with a standard furnace [8]

### (b) Thermographic Approach

The thermography techniques were used during the DMTA measurements to observe the temperature variations of the sample during the cyclic loading. The pixel-to-pixel calibration [9] was performed for each temperature for the Infrared (IR) camera (CEDIP SC7000 series) before using it on the DMTA tests as the temperature variations induced by material deformation might be very small. The IR camera was used during DMTA tests for few frequencies like 0.1 and 1Hz at each temperature of  $25^{\circ}$ ,  $50^{\circ}$  and  $75^{\circ}\text{C}$ . The experimental setup is shown in Figure 2. A special infrared lens was placed in the home-made door of the furnace to allow weakly attenuated infrared assessments. Moreover, two samples were placed, inside the furnace, in the vision field of the camera, one under pulsation and the other (reference sample) to observe the small thermal fluctuations induced by the furnace regulation system.

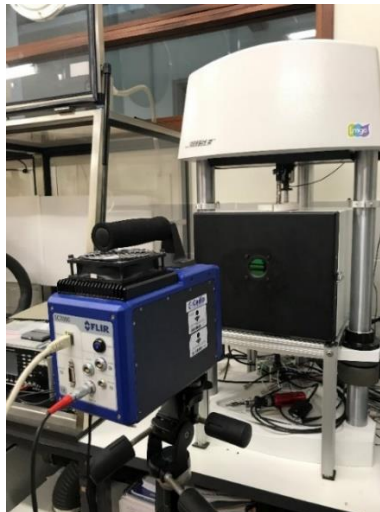


Fig.2 Extended DMTA measurements where the furnace door was equipped with a special infrared transparent window

## Results and Discussion

### (a) Standard DMTA results

The DMTA results on PS are shown in Figures 3a and 3b for several temperatures in the range mentioned previously, where the storage moduli ( $E'$ ) and loss tangents ( $\tan \delta$ ) were plotted against logarithmic frequency. The plots of  $E'$  and  $\tan \delta$  do not include the rubbery state regions since the chosen temperature remained below the glass transition temperature and chosen frequency was not enough to show the relaxation near the glass transition of PS.

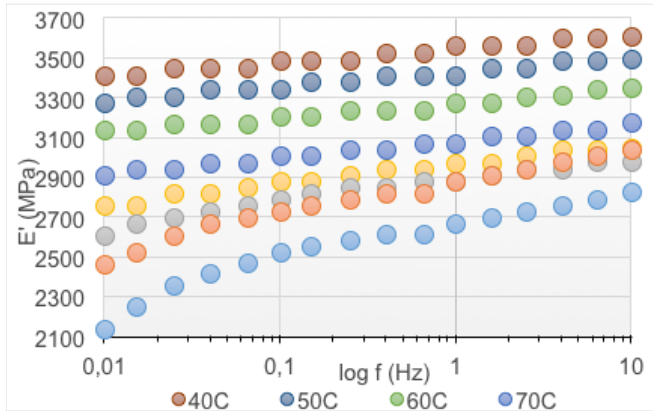


Fig.3a:Storage modulus vs frequency

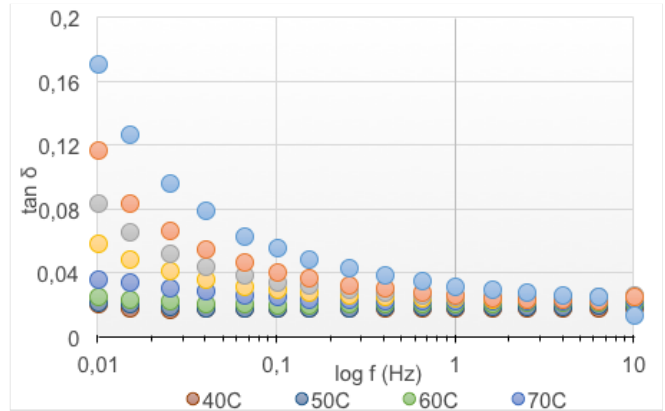


Fig.3b: Loss tangent vs frequency

The results obtained from the frequency sweep measurements were in accordance with the results of the literature as in the evolution of storage moduli was observed to be increasing with the frequency but contrarily decreasing with the increasing temperature. Whereas, in case of loss tangent, it was observed to be inverse of the evolution of storage modulus i.e., decreasing with the increasing frequency but increasing with the temperature.

As it is traditionally done, the frequency sweep results plotted in figure 3(a) and 3(b) obtained at several temperatures were shifted manually by a shift factor ( $a_T$ ) along the frequency scale to get the master curves i.e., the horizontal shift factor was applied to get the master curve at reference temperature 90°C. The master curve obtained after horizontal shift are shown in Figure 4(a) and 4(b).

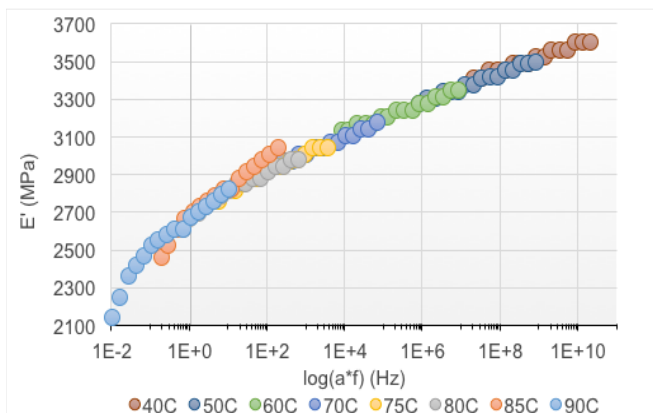


Fig.4(a) Master curve for  $E'$  with horizontal

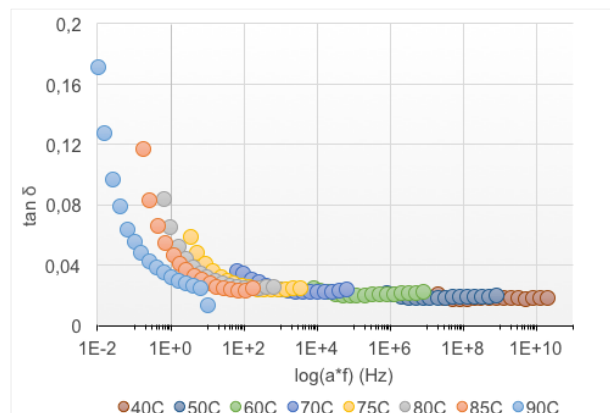


Fig.4(b) Master curve for  $\tan \delta$  with horizontal shift

The application of horizontal shift to build the master curve leads us to the observation that the superposition by displacement along the frequency scale alone cannot yield a master curve in case of loss tangent. A small vertical shift ( $b_T$ ) has also been applied to improve the quality of the  $\tan \delta$  master curve as shown in Figure 5. This vertical shift is legitimated invoking the concept of free volume [10]. Physically, this vertical shift is defined by Equation 3:

$$b_T = \frac{T_0 \rho_0}{T \rho} \quad (3)$$

where  $\rho_0$  and  $\rho$  are respectively the mass density at  $T_0$  and  $T$ .

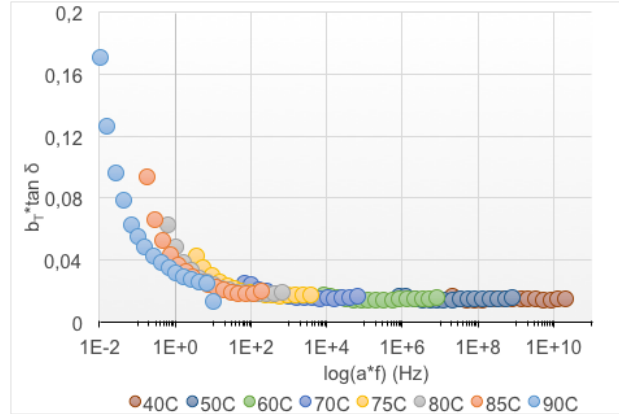


Fig.5 Master curve for  $\tan \delta$  with both shift factors

### (b) Discussion about the Time-Temperature Superposition principle

The previous construction of the master curve leads us to the concept of TTSP that could be expressed by the following assertion: for a given viscoelastic behaviour at “low” temperature and “low” loading frequency, there exists an equivalent behaviour at “high” temperature and “high” frequency. In other words, this behavioural equivalence can be mathematically defined by:

$$\begin{cases} E'(T_0, \omega_0) = E'(T, \omega) \\ E''(T_0, \omega_0) = E''(T, \omega) \end{cases} \quad (4)$$

where  $(T_0, \omega_0)$  represents the couple at “low” temperature and pulsation and  $(T, \omega)$  the couple at “high” temperature and pulsation.

Now, let us consider a generalized form of linear viscoelastic model (generalized Maxwell model [4]) made of  $n+1$  branches, the mathematical expressions of the dynamic moduli  $E'$  and  $E''$  can be written as:

$$E' = E_0 + \sum_{i=1}^n \frac{E_i \tau_i^2 \omega^2}{1 + \tau_i^2 \omega^2} \quad (5)$$

$$E'' = \sum_{i=1}^n \frac{E_i \tau_i \omega}{1 + \tau_i^2 \omega^2} \quad (6)$$

where, index “ $i$ ” refers to each branch,  $E_i$  being the elastic modulus of the  $i^{\text{th}}$  branch and  $\tau_i$  its temperature dependent relaxation time. For such moduli expressions, if we now apply the TTSP consequences (equation 4), we must have:

$$E' = E_0 + \sum_{i=1}^n E_i(T, \omega) \frac{\tau_i^2(T) \omega^2}{1 + \tau_i^2(T) \omega^2} = E_0 + \sum_{i=1}^n E_i(T_0, \omega_0) \frac{\tau_i^{02} \omega_0^2}{1 + \tau_i^{02} \omega_0^2} \quad (7)$$

$$E'' = \sum_{i=1}^n E_i(T, \omega) \frac{\tau_i(T) \omega}{1 + \tau_i^2(T) \omega^2} = \sum_{i=1}^n E_i(T_0, \omega_0) \frac{\tau_i^0 \omega_0}{1 + \tau_i^{02} \omega_0^2} \quad (8)$$

where  $E_0$  corresponds to the elastic modulus of a pure elastic branch and  $\tau_i^0 = \tau_i(T_0)$ . As it is known that elasticity is rate independent, if we admit that  $E_0$  is also temperature independent, or if we do not consider any pure elastic branch in the generalized Maxwell model, the Equations (7,8) will be verified, if, for each branch ‘ $i$ ’ (sufficient condition), we impose:

$$\begin{cases} E_i(T, \omega) \frac{\tau_i^2(T) \omega^2}{1 + \tau_i^2(T) \omega^2} = E_i(T_0, \omega_0) \frac{\tau_i^{02} \omega_0^2}{1 + \tau_i^{02} \omega_0^2} & (a) \\ E_i(T, \omega) \frac{\tau_i(T) \omega}{1 + \tau_i^2(T) \omega^2} = E_i(T_0, \omega_0) \frac{\tau_i^0 \omega_0}{1 + \tau_i^{02} \omega_0^2} & (b) \end{cases} \quad (9)$$

Multiplying now Equation 9b by  $\tau_i^0 \omega_0$ , we obtain:

$$E_i(T, \omega) \frac{\tau_i(T) \omega}{1 + \tau_i^2(T) \omega^2} \times \tau_i^0 \omega_0 = E_i(T, \omega) \frac{\tau_i^2(T) \omega^2}{1 + \tau_i^2(T) \omega^2} \quad (10)$$

Finally, if  $E_i(T, \omega) > 0$ , Equation 10 leads to  $\tau_i(T) \omega = \tau_i(T_0) \omega_0$ , whatever the relaxation time spectrum and its temperature evolution.

In order to get the correspondence between  $(T, \omega)$  and  $(T_0, \omega_0)$  satisfying Equations (7,8), it is sufficient to introduce a unique function  $a_T$ , so that:

$$\tau_i(T) = \frac{\tau_i(T_0)}{a_T(T)} \text{ and then } \omega = a_T(T) \omega_0 \quad (11)$$

In Equation 11, we recognize the characteristics of so called Thermo-rheologically simple material.

### (c) Thermographic results

Thermographic recordings were performed during the DMTA tests at certain temperatures and frequencies to observe the thermo-mechanical couplings and dissipative effects. As mentioned previously, two different samples were used during thermography where one sample was used to observe the regulation of the furnace temperature (dummy specimen). Henceforth, the mean temperature over the central surface of the sample was considered and was subtracted to the mean temperature over a central surface of a reference sample, in order to minimize the disturbing effects of temperature fluctuations of the furnace. In such conditions, we considered that the observed temperature variation was the one of the specimen under loading at an arbitrarily thermal constant. The monotonous increase of these temperature variations can then be associated with the existence of dissipation, while, periodic oscillation corresponds to thermoelastic effects. Using this thermal data, it was also possible to compute the hysteresis area associated with thermo-elastic couplings and estimate the mean dissipation per cycle during the test.

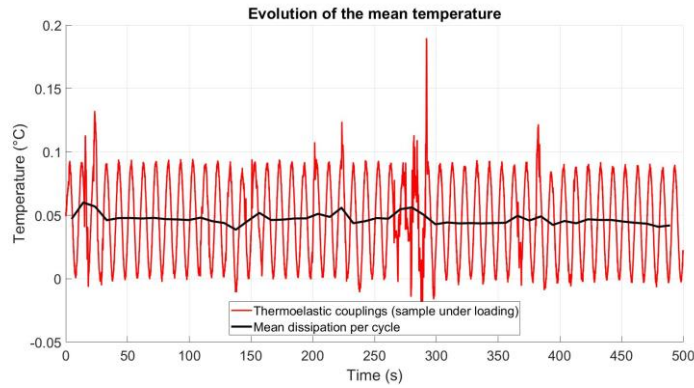


Fig.6 Thermo-elastic couplings at 25°C and 0.1Hz

Some thermographic results were shown in Figures (6,7) in order to highlight the effect of increasing frequency and the furnace temperature on the proper temperature variation of the sample. In the Figures (6,7), it is reminded that the origin of the temperature axis remains arbitrary and that only the oscillation range (thermoelastic effects) and the overall drift (self-heating) have to be taken into account.

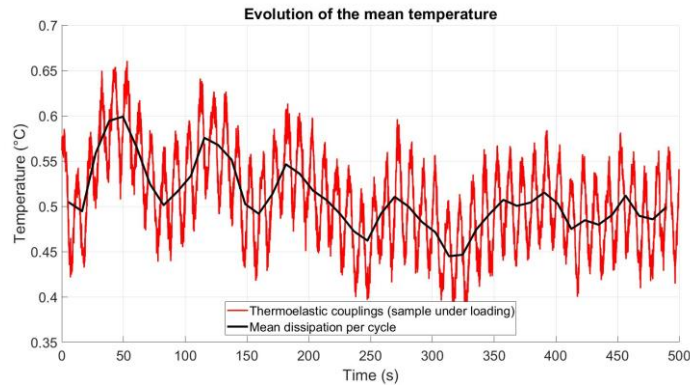


Fig.7 Thermo-elastic couplings at 75°C and 0.1Hz

Despite the narrowness of the temperature variation, Figures (6,7) clearly show the presence of the temperature oscillation while any self-heating of the specimen was difficult to observe. These results are in accordance as it was found in [11], for PMMA and PC specimens. This observation of thermoelastic coupling, during the DMTA tests at low frequencies also made a question mark on the viscous origin of loss modulus, which is assumed to be the result of energy dissipation. That's the reason why we computed the hysteresis area in Table 1 for the different loading frequencies and furnace temperature used during the tests.

Table 1. Derived hysteresis area

Frequency(Hz)	Temperature(°C)	Raw DMTA data ( $A_h$ )	Loss modulus ( $A_{HL}$ )	Thermoelastic couplings ( $A_{the}$ )
0.1	25	224.6	224.5	1.2556
	50	215.0	214.6	2.0735
	75	319.4	319.4	31.4174
1	25	216.6	213.8	6.7146
	50	199.1	198.2	2.1245
	75	271.6	270.5	1.2013



The hysteresis area was first calculated using the stress-strain data given by the DMTA device:

$$A_h = \oint_{\text{cycle}} \sigma \cdot \dot{\epsilon} dt \quad (12)$$

The hysteresis area was then computed using its relation with the loss modulus:

$$A_{HL} = \pi E'' \varepsilon_0^2 \quad (13)$$

We finally estimated the hysteresis area induced by the thermoelastic effects following the equation:

$$A_{the} = -E' \alpha \theta_0 \varepsilon_0 \pi \sin \delta \quad (14)$$

where,  $\alpha$  represents the coefficient of thermal expansion.

Fortunately, the results of column 3 and 4 (Table 1) are consistent. This consistency shows that the numerical scheme integration of the hysteresis area was correctly performed as the identification of the loss modulus using the least square fitting method. The results of column 5 show that the hysteresis area induced by thermoelastic effects remains low compared to the mechanical hysteresis area. The origin of this hysteresis area may be attributed to either dissipation or stored energy variations induced by microstructural transformation during the loading cycles. In this last case, the mechanical cycle cannot be longer a thermodynamic cycle.

If we finally associate the hysteresis area with only dissipative mechanisms, a temperature drift can be computed using the following simplified heat diffusion equation (Eq.15), [12].

$$\dot{\theta} + \frac{\theta}{\tau_{th}} = A_h f / \rho C_p \quad (15)$$

Where  $A_h f$  represents the mean dissipation per cycle,  $\tau_{th}$  a time constant related to the heat losses,  $\rho$  and  $C_p$  the mass density and specific heat capacity of the material. In each case, the temperature drift remained less than 1/100°C which is currently experimentally unreachable via IR techniques.

## Concluding comments

1. The narrowness of the temperature variation of the specimen during the DMTA tests legitimates the assumption that the temperature imposed by the furnace can be considered as the temperature of the sample (very small self-heating) which is in agreement with the DMTA protocol. In such conditions, the sample temperature is then a controlled parameter
2. Nevertheless, small temperature oscillations were observed, which lead us to wonder about the pure viscous origin of the loss modulus. The computation of the thermoelastic hysteresis area showed that latter remains small compared to the mechanical one.
3. Conversely, we computed the asymptotic self-heating temperature induced by the entire hysteresis area assuming its dissipated origin. In all observed cases, the temperature variations remained under the thermal resolution of the camera.
4. At this level, it is then impossible to confirm the dissipative origin of the hysteresis area that could also be generated by the stored energy variations.

## Perspectives

The further study about this discussion has to be done by strengthen our experimental database. In particular, polyamide samples are to be tested in a near future. We already know [13] that this material is strongly dissipative even if its cyclic deformation is accompanied by non negligible coupling effects.

Besides, the identification of thermo-visco-elastic Maxwell model is underway. This model will be constructed within the framework of 'generalized standard material' framework [6] considering the temperature of the specimen as a state variable and not a controlled parameter. The first step is to construct the relaxation time spectra at different temperatures using the  $E'$  and  $E''$  assessments. Finally, the viscoelastic and thermo-elastic effects will be compared using numerical simulations.

## References

- [1] Menard KP, Dynamic mechanical analysis: a practical introduction, Taylor & Francis Group, Texas, 2008.
- [2] Seitz JT, Balazs CF, Application of time-temperature superposition principle to long term engineering properties of plastic materials, *Polymer Engineering & Science*, vol. 8, 151-160, 1968.
- [3] Patel M, Viscoelastic properties of polystyrene using dynamic rheometry, *Polymer testing* 23(1), 107-112, 2004.
- [4] Ferry JD, *Viscoelastic properties of polymers*, John Wiley & Sons, New York, 1980.
- [5] Zener C, Internal friction in solids I. Theory of internal friction in reeds, *Physical Review Journal*, vol. 52, 230-235, 1937.
- [6] Chrysochoos A, Thermomechanical analysis of the cyclic behavior of materials, *Procedia IUTAM* 4, 15-26, 2012.
- [7] Paolo Lomellini, Viscosity-temperature relationships of a polycarbonate melt: Williams-landel-ferry versus Arrhenius behaviour, *Macromolecular Chemistry and Physics* 193(1), 69-79, 1992.
- [8] <https://www.tainstruments.com/products/electroforce-mechanical-testers>.
- [9] Honorat V, Moreau S, Muracciole JM, Wattrisse B and Chrysochoos A, Calorimetric analysis of polymer behaviour using a pixel calibration of an IRFPA camera, *Quantitative InfraRed Thermography Journal*, 2(2), 153-171, 2012.
- [10] Capodagli J and Lakes R, Isothermal viscoelastic properties of PMMA and LDPE over 11 decades of frequency and time: a test of time-temperature superposition, *Rheological Acta* 47, 777-786, 2008.
- [11] Moreau S, Chrysochoos A, Muracciole JM and Wattrisse B, Analysis of thermoelastic effects accompanying the deformation of PMMA and PC polymers, *Elsevier Masson*, 333(8), 648-653, 2005.
- [12] Chrysochoos A., Louche H., An infrared image processing to analyse the calorific effects accompanying strain localisation, *Internal Journal of Engineering Science*, 38, 16, 1759-1788, 2000.
- [13] Benaarbia A., Chrysochoos A., Robert G., Thermomechanical analysis of the onset of strain concentration zones in wet polyamide 6.6 subjected to cyclic loading, *Mechanics of Materials*, 99, 9-25, 2016.